Advances in SAR Remote Sensing of Oceans

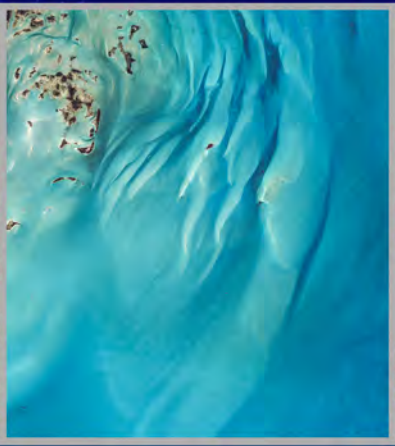

Edited by
Xiaofeng Li · Huadong Guo
Kun-Shan Chen · Xiaofeng Yang

CRC Press
Taylor & Francis Group

14 Oceanographic Aspect of Tropical Cyclone Wind and Wave Remote Sensing

Paul A. Hwang, Yalin Fan, Xiaofeng Li, and Weizeng Shao

CONTENTS

14.1 INTRODUCTION

There are two major components in ocean remote sensing: remote sensing and oceanography. The former deals primarily with the science and technology of acquiring data, and covers diverse subjects from hardware to the electromagnetic (EM) aspects of the issue. The latter is primarily about interpreting the ocean processes revealed from the received signal.

Take microwave wind remote sensing as an example, the sensors, e.g., scatterometer, altimeter, microwave radiometer, synthetic aperture radar (SAR) used as a fine-resolution scatterometer, Global Navigation Satellite System Reflectometry (GNSS-R), are touted as operational in all-weather and day-and-night conditions, thus they are through-cloud and through-air. Yet, the product of wind velocity from these microwave sensors are the motion of the air that is supposed to be transparent to the sensors.

The oceanographic explanation of the apparently paradoxical outcome is the strong correlation between wind and surface waves, and that the EM signals emitted or scattered to the microwave sensors are from the surface waves at the air-sea interface. These EM signals: brightness temperature T_B in the case of radiometer and normalized radar cross section (NRCS) σ_0 in the case of radars serving in active (e.g., scatterometer, altimeter, SAR) or passive (e.g., GNSS-R) mode of the sensing

systems, are modified by the surface roughness conditions at the air-sea interface. Because wind is the dominant driving force of the surface roughness variation, thus T_B or σ_0 can be used to derive wind properties.

The sensor systems discussed in the last paragraph make use of the wind and wave correlation in small-scale ocean surface waves much shorter than the energy-containing dominant waves near the wave energy spectral peak region. The physical mechanisms governing the kinematics and dynamics of short waves far away from the wave spectral peak region remain poorly quantified. So far there is no agreement on the spectral function of these roughness-contributing short scale waves and many roughness spectral models exist with very different relationships between the roughness components and the wind velocity.

In contrast to the short scale waves, the correlation between wind and waves in the energy-containing spectral components is on a much more solid foundation. The concept of fetch- and duration-limited wind wave growth was established even before the World War II period, as clearly summarized in the report by Sverdrup and Munk (1947). Our understanding of the wind-wave growth has been enriched by many subsequent theoretical studies, numerical simulations, as well as field and laboratory experiments.

Recent analyses show that for hurricane conditions, the wind and dominant wave parameters are also governed by the fetch- and duration-limited principle, and the wind-wave growth functions developed for steady wind forcing conditions can be applied to the wave development inside hurricanes (Young 1998, 2006, 2017; Hwang 2016; Hwang and Walsh 2016; Hwang and Fan 2017). The fetch- or duration-limited wave growth functions are made up of a pair of equations describing the growth of wave height and wave period as a function of wind speed for a given fetch or duration.

With the two equations connecting the significant wave height H_s, dominant wave period T_p, and surface wind speed U_{10}, the full set of wind-wave triplets (U_{10}, H_s, and T_p) can be derived knowing any one of the three. This property can be exploited for remote sensing of winds and waves inside tropical cyclones.

In the following, Section 14.2 describes the fetch- and duration-limited wind-wave growth, with emphasis on retrieving the full set of the wind-wave triplets knowing only one of the three members. Section 14.3 gives examples of remote sensing applications to derived the sea state parameters (H_s and T_p) from wind input (U_{10}) or vice versa. Section 14.4 is summary.

14.2 ENABLING SCIENTIFIC PRINCIPLE: FETCH- AND DURATION-LIMITED WAVE GROWTH

Wind-generated wave growth at a given fetch or duration can be expressed as a pair of dimensionless equations describing the growth of wave height and wave period subject to wind forcing. Many sets of growth functions have been proposed over the years (e.g., Hasselmann et al. 1973, 1976; Donelan et al. 1985; Hwang and Wang 2004). Hwang and Wang (2004) obtain the first and second order fittings of data assembled from five field experiments under steady wind forcing and near-neutral stability conditions (Burling 1959; Hasselmann et al. 1973; Donelan et al. 1985;

Dobson et al. 1989; Babanin and Soloviev 1998). In addition to expanding the parameter range by combining many datasets, they describe a mathematical connection between fetch, duration, and wave-age similarities. The mathematical connection makes it feasible to use the more abundant and better quality fetch-limited experimental results to fill in gaps in the rarely occurred and difficult-to-acquire duration-limited experiments, especially for the early stage of wave development. Their functions for fetch, duration, and wave-age similarity relationships are all derived from the combined field data. The first order fitting equations are:

$$\begin{aligned} \eta_{\#} &= 6.19\times10^{-7} x_{\#}^{0.81};\ \omega_{\#} = 11.86 x_{\#}^{-0.24} \\ \eta_{\#} &= 1.27\times10^{-8} t_{\#}^{1.06};\ \ \omega_{\#} = 36.92 t_{\#}^{-0.31}. \end{aligned} \tag{14.1}$$

The dimensionless parameters are given as $\eta_{\#} = \eta_{rms}^2 g^2 U_{10}^{-4} = H_s^2 g^2 \left(16U_{10}^4\right)^{-1}$, $\omega_{\#} = 2\pi U_{10}\left(T_p g\right)^{-1}$, $x_{\#} = x_f g U_{10}^{-2}$, $t_{\#} = t_d g U_{10}^{-1}$ and η_{rms}^2 is the variance of the ocean surface displacement, g is gravitational acceleration, x_f and t_d are effective fetch and duration, respectively.

Keeping the wind-wave triplets (U_{10}, H_s, T_p) explicitly in the equations, the fetch-limited condition can be expressed as

$$\frac{H_s^2 g^2}{16U_{10}^4} = 6.19\times10^{-7}\left(\frac{x_f g}{U_{10}^2}\right)^{0.81}, \qquad \frac{2\pi U_{10}}{T_p g} = 11.86\left(\frac{x_f g}{U_{10}^2}\right)^{-0.24}. \tag{14.2}$$

Similarly, for the duration-limited condition

$$\frac{H_s^2 g^2}{16U_{10}^4} = 1.27\times10^{-8}\left(\frac{t_d g}{U_{10}}\right)^{1.06}, \qquad \frac{2\pi U_{10}}{T_p g} = 2.94\left(\frac{t_d g}{U_{10}}\right)^{-0.34}. \tag{14.3}$$

The two similarity equations facilitate the determination of the full set of the wind-wave triplets given only one of the three as input. In the conventional application of the wave growth functions, the fetch or duration is a known quantity. Typically, these equations are used to obtain wave information (H_s and T_p) from wind input for given distances from shore or for some time intervals after the start of a wind event in an unbounded water body. Indeed, they provide wave forecast/hindcast prior to the advent of numerical wave models, and after numerical wave models become prevalent the fetch- and duration-limited wave growths are important benchmark tests for fine-tuning the various source and sink functions of the wave energy or action equation.

To determine the effective fetch and duration of a tropical cyclone wind field, Hwang and Fan (2017) describe a reverse engineering procedure making use of the simultaneous wind and wave measurements from four hurricane reconnaissance missions during Bonnie 1998 (Wright et al. 2001) and Ivan 2004 (Fan et al. 2009). These airborne missions supply the wind-wave triplets (U_{10}, H_s, T_p) with precise radial and azimuthal information of the locations where the measurements were made. Figure 14.1 shows the four sets of data: one (B24) from Bonnie 1998 and three (I09, I12, and I14)

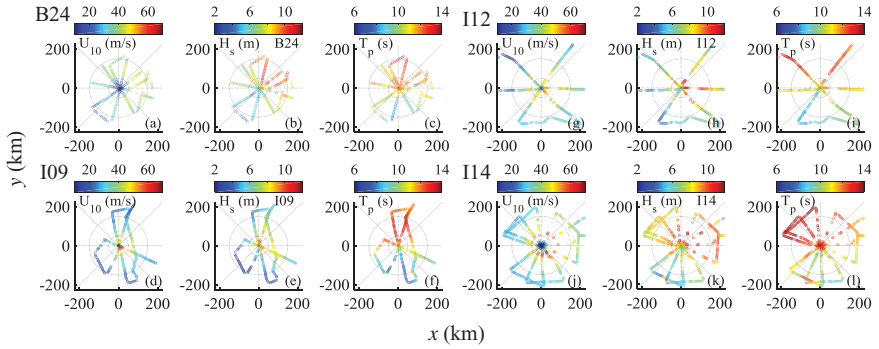

FIGURE 14.1 Simultaneous wind and wave measurements from four hurricane reconnaissance missions; these datasets are denoted B24, I09, I12, and I14.

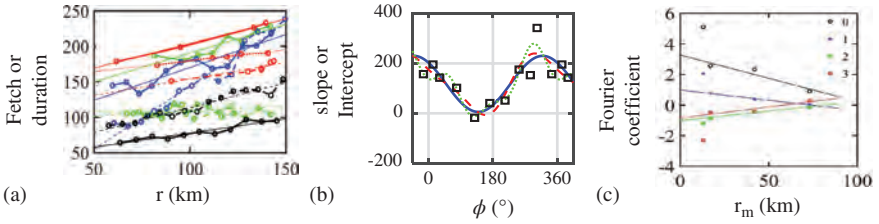

FIGURE 14.2 (a) The fetch or duration data along each radial transect show linear dependence on the distance r from the hurricane center, (b) The azimuthal variation of the slope and intercept can be represented by Fourier series, and (c) The Fourier coefficients are dependent on a small number of characteristic hurricane parameters, an example of the dependence on r_m. (From Hwang, P.A. and Fan, Y., *J. Phys. Oceanogr.*, 47, 447–470, 2017.) is illustrated.

from Ivan 2004. The coordinates in this figure have been rotated such that the hurricane heading is in the +y direction (toward the top of the page).

With the wind-wave triplets available, fetch or duration becomes the only unknown in the wind-wave growth functions and it can be derived from Equations (14.2) or (14.3). Figure 14.2 presents examples illustrating the reverse engineering procedure:

a. Processing the fetch or duration data along each radial transect, the result shows linear dependence on the distance r from the hurricane center, analogous to a circular race track:

$$x_f(r,\phi) \text{ or } t_d(r,\phi) = s(\phi)\cdot r + I(\phi). \tag{14.4}$$

b. The azimuthal variation of the slope s and intercept I can be represented by Fourier series, in consideration of the azimuthal cyclical and continuous nature:

$$q = a_{0,q} + 2\sum_{n=1}^{N}\left(a_{n,q}\cos n\phi + b_{n,q}\sin n\phi\right), q = s \text{ or } I. \tag{14.5}$$

c. The Fourier coefficients are dependent on a small number of characteristic hurricane parameters:

$$a_n \text{ or } b_n = f\left(\text{hurricane parameters}\right). \tag{14.6}$$

Steps (a) and (b) represent a very efficient distillation process to reduce the number of variables characterizing the hurricane wind field. For example, at 5 km spatial resolution a hurricane coverage area 500 km each side would contain 10000 fetch or duration values. Step (a) reduces each azimuthal transect into two numbers (slope and intercept), and step (b) further reduces those slopes and intercepts into a small number of Fourier coefficients. Our analysis of the hurricane reconnaissance data shows that the slope or intercept results can be sufficiently represented by a three-harmonic Fourier series. So the 10000 fetch or duration values are condensed to two sets of 7 Fourier coefficients for the slopes and intercepts of the radial dependence. This condensing procedure makes it feasible for quantifying the fetch or duration of the hurricane wind field by a small number of the characteristic hurricane parameters in step (c).

Limited by the small number of the hurricane reconnaissance datasets, the fetch and duration model of Hwang and Fan (2017) has only one hurricane parameter r_m: the radius of maximum wind speed; the detail is provided in their Section 14.3.

Other important hurricane parameters discussed in the literature include the hurricane translation speed V_h and hurricane intensity (maximum wind speed) $U_{10\max}$ (e.g., Young 1988; Young and Burchell 2006; Young and Vinoth 2013). The three fetch models by Young and colleagues specify a constant fetch for each hurricane, so the spatial variation of the wave field reflects simply the spatial variation of the wind field. The hurricane reconnaissance wind and wave data, however, show considerable difference in the spatial patterns of U_{10}, H_s, and T_p; see discussions in Section 14.4e of Hwang and Fan (2017).

Figure 14.3 shows the comparison of hurricane and non-hurricane datasets of wind speed, wave height, and wave period presented in fetch- and duration-limited growth functions. The non-hurricane data are assembled from many decades of field experiments as described in Hwang and Wang (2004). The hurricane data are the combined four hurricane reconnaissance missions as described in Hwang and Fan (2017). The non-hurricane data are shown with light-colored symbols, the hurricane data are divided into three groups in different sectors of the hurricane coverage area: black right-pointing triangles for the right half-plane (r = 50 to 200 km), blue left-pointing triangles for the inner region (r = 50 to 100 km) of the left half-plane, and red left-pointing triangles for the outer region (r = 100 to 200 km) of the left half-plane. Both hurricane and non-hurricane measurements show similar degree of data scatter and they can be described by the same set of wind-wave growth functions: the solid curves represent the second order fitting equations and the dashed curves are the first order fitting Equations (14.1) or (14.2)–(14.3).

With the effective fetch or duration given by the scale model, the full set of the wind-wave triplets (U_{10}, H_s, T_p) can be obtained given any one of the three measured. This is of great value for remote sensing of tropical cyclones. A couple of examples are discussed in the next section.

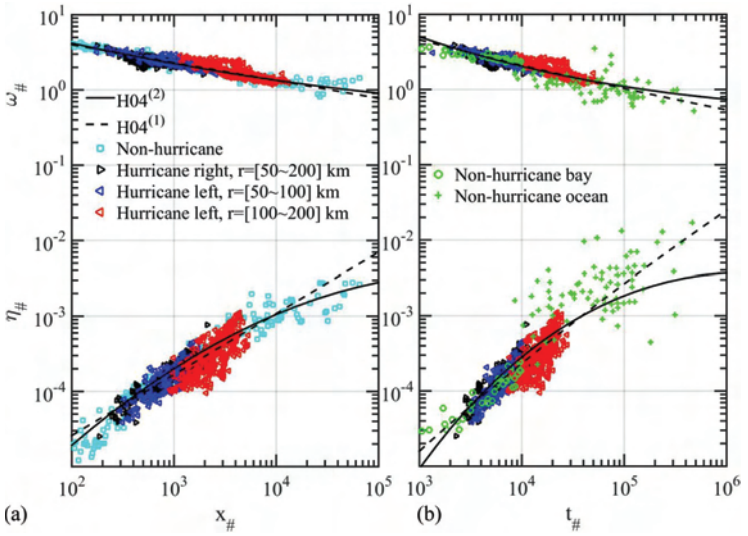

FIGURE 14.3 Comparison of hurricane and non-hurricane wind and wave data presented in terms of the (a) fetch-limited growth functions: $\eta_{\#}(x_{\#})$ and $\omega_{\#}(x_{\#})$, and (b) duration-limited growth functions: $\eta_{\#}(t_{\#})$ and $\omega_{\#}(t_{\#})$. The non-hurricane data are shown with light-colored symbols, the hurricane data are divided into three groups in different sectors of the hurricane coverage area: black right-pointing triangles for the right half-plane ($r = 50$ to 200 km), blue left-pointing triangles for the inner region ($r = 50$ to 100 km) of the left half-plane, and red left-pointing triangles for the outer region ($r = 100$ to 200 km) of the left half-plane.

14.3 APPLICATION TO REMOTE SENSING OF TROPICAL CYCLONES

14.3.1 Deriving Wave Properties from Wind Input

Among the three wind-wave parameters, wind sensing is operationally the most advanced. Presently there is no comprehensive operational sea state remote sensing capability over the global scale. Making use of the wind-wave growth nature of hurricane waves, we can at least provide the sea state information of wave height and wave period using the wind input from the existing wind sensors to enhance global hurricane monitoring.

The sea state retrieval equations for the fetch relation are

$$H_s = 8.10\times10^{-4}U_{10}^{1.19}x_{\eta x}^{0.405}$$
$$T_p = 9.28\times10^{-2}U_{10}^{0.526}x_{\omega x}^{0.237}. \tag{14.7}$$

Similarly, for the duration relation,

$$H_s = 1.55\times10^{-4}U_{10}^{1.47}t_{\eta t}^{0.531}$$
$$T_p = 3.53\times10^{-2}U_{10}^{0.690}t_{\omega t}^{0.310}. \tag{14.8}$$

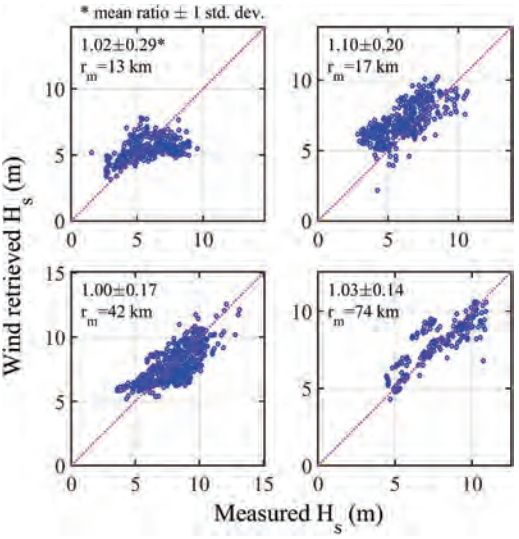

FIGURE 14.4 Significant wave height derived from wind input using the fetch relation applied to four hurricane reconnaissance datasets. The statistics of the average ratio of retrieved and measured wave height with one standard deviation for each dataset is shown at the top-line text in each panel. The radius of maximum wind is shown in the second-line text.

Hwang and Fan (2017) assign different fetch and duration for wave height and wave period to account for the observed systematic deviation from the ideal growth function in different azimuthal regions inside the hurricane coverage area, as discussed in Hwang and Walsh (2016). The distinction is denoted by the dual subscripts of fetch x_{ij} or duration t_{ij}. For example, subscripts ηx and ωx indicate that the associated variables are applicable to $\eta_{\#}(x_{\#})$ and $\omega_{\#}(x_{\#})$, respectively.

An example of deriving the wave height from wind input using the fetch relation is shown in Figure 14.4. The four sets of hurricane reconnaissance measurements are used for this illustration. The horizontal axis is the measured significant wave height, and the vertical axis is the retrieved wave height with wind speed and fetch. The statistics of the average ratio of retrieved and measured wave heights with one standard deviation for each dataset is shown at the top-line text in each panel. The radius of maximum wind is shown in the second-line text.

Overall, the results are very good: the average ratio varies from 1.0 to 1.1, the standard deviation varies from 0.14 to 0.29. There is a tendency of increasing data scatter, as reflected in the magnitude of the standard deviation, toward smaller r_m, which is frequently associated with more intense hurricanes. It is perceivable that further improvement can be expected when additional hurricane parameters such as V_h and $U_{10\max}$ can be incorporated in the fetch and duration scaling model.

14.3.2 Deriving Wind from Wave Input

Active microwave wind sensors (scatterometer, SAR, altimeter, GNSS-R) may suffer signal saturation problem in high wind conditions (e.g., Hwang and Fois 2015).

SAR and altimeter have excellent wave sensing capability and can be exploited for hurricane wind retrieval from wave sensing (Hwang et al. 2017a, 2017b; Shao et al. 2017).

The wind retrieval equations for the fetch relation are

$$U_{10} = 397.46 H_s^{0.841} x_{\eta x}^{-0.341}$$
$$U_{10} = 91.49 T_p^{1.900} x_{\omega x}^{-0.450}. \tag{14.9}$$

Similarly, for the duration relation,

$$U_{10} = 392.95 H_s^{0.681} t_{\eta t}^{-0.362}$$
$$U_{10} = 127.71 T_p^{1.450} t_{\omega t}^{-0.450}. \tag{14.10}$$

An example of derived wind speed from the dominant wavelength input using the fetch relation is shown in Figure 14.5, which reproduced figure 6 of Shao et al. (2017). The results are from processing 9 RADARSAT2 images, each capture a tropical cyclone. The hurricane coverage area is divided into sub-images and the dominant wavelengths of the wave fields are calculated using the algorithm developed by Romeiser et al. (2015). The dominant wavelength is then used to calculate the spectral peak wave period. The tropical cyclone best track information is used to determine the heading for processing the fetch of the wind field. The radius of the maximum wind speed is estimated from the SAR image for computing the fetch at any location inside the tropical cyclone using an earlier version of the fetch scaling model described in Hwang (2016). Combining the fetch information and the spectral perk wave period, the wind speed is derived for each sub-image inside the tropical cyclone where the wave processing is performed. The reference wind speed is from a parameterization model Symmetric Hurricane Estimates for Wind (SHEW) reported in Zhang et al. (2017). The results of comparison in the left, right, and back sectors of the tropical cyclones are shown in Figure 14.5a, b, and c, respectively;

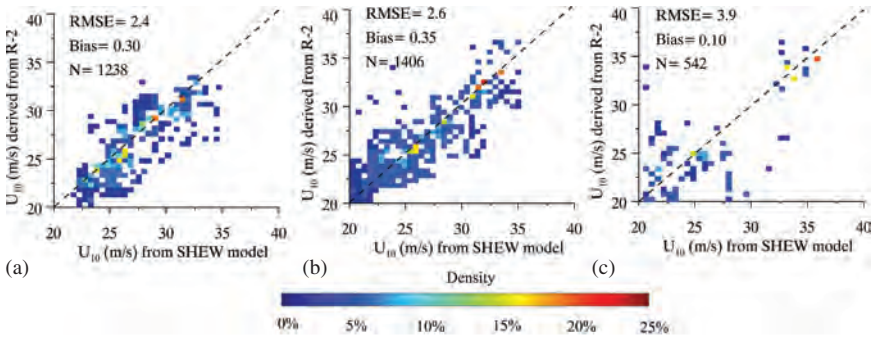

FIGURE 14.5 Wind speed derived from SAR wavelength compared to the SHEW model wind in the (a) left, (b) right, and (c) back sectors of tropical cyclones; reproducing figure 6 of Shao et al. (2017). (From Shao, W. et al., *J. Geophys. Res.*, 122, 6714–6724, 2017.)

the corresponding root mean squares error (RMSE) and bias are (3.9 m/s, 0.1 m/s), (2.4 m/s, 0.3 m/s) and (2.6 m/s, 0.35 m/s).

14.4 SUMMARY

Simultaneous wind and wave data collected in tropical cyclone conditions reveal that the surface wave development inside hurricanes are governed by the same fetch- and duration-limited principles established in steady wind forcing conditions. The pair of equations describing the growth of wave height and wave period subject to wind forcing provides the means to derive the full set of the wind-wave triplets knowing only one of the three. Hwang and Fan (2017) describe a scaling model for specifying the fetch and duration at any location inside a hurricane wind field. Defining the fetch and duration of the hurricane wind field is critical to the application of the wind-wave growth functions for deriving sea state parameters (wave height and wave period) from wind input, or for deriving hurricane wind speed from wave parameters (Section 14.3).

Because of the small number of datasets (four sets from two hurricanes) available for the scaling model development, in its present form, the radius of maximum wind speed is the only hurricane parameter in the scaling model. Literature survey indicates that hurricane translation speed and hurricane intensity are also important factors influencing the effective fetch or duration. Further improvement in performance can be expected when larger datasets can be assembled for incorporating additional hurricane parameters in the fetch and duration scaling model.

REFERENCES

Babanin, A.V., and Y. P. Soloviev, 1998: Field investigation of transformation of the wind wave frequency spectrum with fetch and the stage of development. *J. Phys. Oceanogr.*, 28, 563–576.

Burling, R. W., 1959: The spectrum of waves at short fetches. *Dtsch. Hydrogr. Z.*, **12**, 96–117.

Dobson, F., W. Perrie, and B. Toulany, 1989: On the deep-water fetch laws for wind-generated surface gravity waves. *Atmos.-Ocean*, **27**, 210–236.

Donelan, M. A., J. Hamilton, and W. H. Hui, 1985: Directional spectra of wind-generated waves, *Phil. Trans. Roy. Soc. Lond.*, **A315**, 509–562.

Fan, Y., I. Ginis, T. Hara, C. W. Wright, and E. J. Walsh, 2009: Numerical simulations and observations of surface wave fields under an extreme tropical cyclone. *J. Phys. Oceanogr.*, **39**, 2097–2116.

Hasselmann, K. et al. 1973: Measurements of wind-wave growth and swell decay during the Joint North Sea Wave Project (JONSWAP). *Deutsch. Hydrogr. Z.*, Suppl. **A8(12)**, 95.

Hasselmann, K., D. B. Ross, P. Müller, and W. Sell, 1976: A parametric wave prediction model. *J. Phys. Oceanogr.*, **6**, 200–228.

Hwang, P. A., 2016: Fetch- and duration-limited nature of surface wave growth inside tropical cyclones: With applications to air-sea exchange and remote sensing. *J. Phys. Oceanogr.*, **46**, 41–56. doi:10.1175/JPO-D-15-0173.1.

Hwang, P. A., and D. W. Wang, 2004: Field measurements of duration limited growth of wind-generated ocean surface waves at young stage of development. *J. Phys. Oceanogr.*, **34**, 2316–2326. (Corrigendum, **35**, 268–270, 2005).

Hwang, P. A., and F. Fois, 2015: Surface roughness and breaking wave properties retrieved from polarimetric microwave radar backscattering. *J. Geophys. Res.*, **120**, 3640–3657. doi:10.1029/2015JC010782.

Hwang, P. A., and E. J. Walsh, 2016: Azimuthal and radial variation of wind-generated surface waves inside tropical cyclones. *J. Phys. Oceanogr.*, **46**, 2605–2621. doi:10.1175/JPO-D-16-0051.1.

Hwang, P. A., and Y. Fan, 2017: Effective fetch and duration of tropical cyclone wind fields estimated from simultaneous wind and wave measurements: Surface wave and air-sea exchange computation. *J. Phys. Oceanogr.*, **47**, 447–470. doi:10.1175/JPO-D-16-0180.1.

Hwang, P. A., X. Li, and B. Zhang, 2017a: Retrieving hurricane wind speed from dominant wave parameters. *IEEE J. Sel. Topics Appl. Earth Obs. Rem. Sens.*, **10**(6), 2589–2598. doi:10.1109/JSTARS.2017.2650410.

Hwang, P. A., X. Li, and B. Zhang, 2017b: Coupled nature of hurricane wind and wave properties for ocean remote sensing of hurricane wind speed. In *Hurricane Monitoring With Spaceborne Synthetic Aperture Radar*, (Ed.) X. Li, Springer Natural Hazards, pp. 215–236, Springer Nature, Singapore

Romeiser, R., H. C. Graber, M. J. Caruso, R. E. Jensen, D. T. Walker, and A. T. Cox 2015: A new approach to ocean wave parameter estimates from C-band ScanSAR images, *IEEE Trans. Geosci. Remote Sens.*, **53**, 1320–1345. doi:10.1109/TGRS.2014.2337663.

Shao, W., X. Li, P. Hwang, B. Zhang, and X. Yang, 2017: Bridging the gap between cyclone wind and wave by C-band SAR measurements. *J. Geophys. Res.*, **122**, 6714–6724. doi:10.1002/2017JC012908.

Sverdrup, H. U., and W. H. Munk, 1947: Wind, sea, and swell: Theory of relations for forecasting. U. S. Navy Hydrographic Office, *Tech. Rep.* **1**, 56.

Wright, C. W., E. J. Walsh, D. Vandemark, W. B. Krabill, A. W. Garcia, S. H. Houston, M. D. Powell, P. G. Black, and F. D. Marks, 2001: Hurricane directional wave spectrum spatial variation in the open ocean. *J. Phys. Oceanogr.*, **31**, 2472–2488.

Young, I. R. 1988a: Parametric hurricane wave prediction model. *ASCE J. Waterway, Port, Coastal and Ocean Eng.*, **114**, 637–652.

Young, I. R., 1998b: Observations of the spectra of hurricane generated waves. *Ocean Eng.*, **25**, 261–276.

Young, I. R., 2006: Directional spectra of hurricane wind waves. *J. Geophys. Res.*, **111**, C08020, 1–14.

Young, I. R., 2017: A review of parametric descriptions of tropical cyclone wind-wave generation. *Atmosphere*, **8**, 194(1–20).

Young, I. R., and G. P. Burchell, 2006: Hurricane generated waves as observed by satellite. *Ocean Eng.*, **23**, 761–776.

Young, I. R., and J. Vinoth, 2013: An "extended fetch" model for the spatial distribution of tropical cyclone wind-waves as observed by altimeter. *Ocean Eng.*, **70**, 14–24.

Zhang, G., W. Perrie, X. Li, and J. Zhang, 2017: A hurricane morphology and sea surface wind vector estimation model based on C-band cross-polarization SAR imagery. *IEEE Trans. Geosci. Remote Sens.*, **55**, 1743–1751. doi:10.1109/TGRS.2016.2631663.